BURST GEOMAGNETIC PULSATIONS AS INDICATORS OF SUBSTORM EXPANSION ONSETS DURING SUPERSTORMS

Battuulai Tsegmed[1], Vladimir Mishin[2], Julia Klibanova[3], and Marina Kurikalova[4]

[1]Institute of Astronomy and Geophysics, Mongolian Academy of Sciences
[2]Institute of Solar-Terrestrial Physics Siberian Branch of Russian Academy of Sciences
[3]3A. A. Ezhevsky Federal State Budgetary Educational Institute of Higher Education Irkutsk State Agrarian University
[4]Institute of Solar-Terrestrial Physics of Siberian Branch of Russian Academy of Sciences, Irkutsk

November 26, 2022

Abstract

We report on the dynamics of field-aligned currents (FACs), broadband geomagnetic pulsations, and airglow obtained from the Irkutsk (IRK), Mondy (MND), and Borok (BOX) midlatitude geomagnetic observatories and the Tory (TOR) optical Observatory during superstorm substorms. For the first time, using the short duration, [?]t < 0.5 min, high-frequency component of the burst pulsations (Pi1B), we determined the substorm double expansion phase (EP) onsets <5 min apart, which is hardly possible by means of the low frequency (periods of 2–5 min) Psc/PiB pulsations. We argue that the observed burst pulsations are the result of prompt changes in the solar wind dynamic pressure and/or the current circuit related to the westward electrojet. Each pulsed source can excite short bursts of broadband electromagnetic modes of the ionospheric Alfvén resonator in the range of short-period pulsations with a periodic resonance structure of the spectrum characteristic of the observed Pi1B/Psc pulsations

Vladimir Vilenovich Mishin, ORCID: 0000-0002-2729-2862, vladm@iszf.irk.ru
Battuulai Tsegmed, ORCID: 0000-0002-4828-8424, tseg@iag.ac.mn
Yuliya Yurevna Klibanova, ORCID: 0000-0001-7151-3629, malozemova81@mail.ru
Marina Aleksandrovna Kurikalova, ORCID: 0000-0002-0710-8917, kurikalova@iszf.irk.ru

BURST GEOMAGNETIC PULSATIONS AS INDICATORS OF SUBSTORM EXPANSION ONSETS DURING SUPERSTORMS

V.V. Mishin[1], B. Tsegmed[2], Yu.Yu. Klibanova[3], M.A. Kurikalova[1]

[1]Institute of Solar-Terrestrial Physics of Siberian Branch of Russian Academy of Sciences, Irkutsk, Russia (ISTP SBRAS).

[2]Institute of Astronomy and Geophysics, Mongolian Academy of Sciences, Ulaanbaatar, Mongolia.

[3]A. A. Ezhevsky Federal State Budgetary Educational Institute of Higher Education Irkutsk State Agrarian University, Irkutsk, Russia.

Corresponding author: Tsegmed Battuulai, Email: tseg@iag.ac.mn

Postal address: Institute of Astronomy and Geophysics, Mongolian Academy of Sciences, Ulaanbaatar-51, POB-152, Mongolia 13343

Abstract

We report on the dynamics of field-aligned currents (FACs), broadband geomagnetic pulsations, and airglow obtained from the Irkutsk (IRK), Mondy (MND), and Borok (BOX) midlatitude geomagnetic observatories and the Tory (TOR) optical Observatory during superstorm substorms. For the first time, using the short duration, $\Delta t < 0.5$ min, high-frequency component of the burst pulsations (Pi1B), we determined the substorm double expansion phase (EP) onsets <5 min apart, which is hardly possible by means of the low frequency (periods of 2–5 min) Psc/PiB pulsations. We argue that the observed burst pulsations are the result of prompt changes in the solar wind dynamic pressure and/or the current circuit related to the westward electrojet. Each pulsed source can excite short bursts of broadband electromagnetic modes of the ionospheric Alfvén

resonator in the range of short-period pulsations with a periodic resonance structure of the spectrum characteristic of the observed Pi1B/Psc pulsations.

Key points

We explored the dynamics of field-aligned currents, geomagnetic burst pulsations, and airglow during superstorm substorms.

Short duration of the high frequency part of Pi1B pulsation trains allows us to determine the double expansion onsets.

We suggest that prompt changes in the solar wind pressure or/and the westward electrojet generate the two types of the observed pulsations

Key words

substorm, expansion onset, superstorm, field-aligned currents, burst pulsations, auroral emissions

Plain Language Summary

We explored geomagnetic and optical midlatitude observations during superstorms. In addition to the common low frequency (periods of 2–5 min) Psc/PiB pulsations, we used the short period part (Pi1B) of burst pulsations with $T < 10$ s. That allowed us to determine not only isolated substorm expansion onsets but also double substorm onsets and series of onsets of short substorm activations or pseudobreakups during storms. This is hardly possible with the commonly used long-period pulsations (Pi2, Pi3) is problematic due to their long duration

1. Introduction

Magnetic storms are a global phenomenon that greatly disturbs the space environment near the Earth. A typical major storm lasts for several days. During this disturbed period, occurring intermittently magnetospheric substorms create abrupt intensifications of optical (auroral) emissions and electric fields and currents in the high- and mid-latitude ionosphere (Akasofu, 1964; Tinsley, 1986; Brunelli, 1988; Rassoul et al., 1993; Mikhalev, 2013; V.V. Mishin et al., 2018, Klibanova et al., 2019). A typical substorm comprises the growth phase, explosive (active or expansion) phase, and recovery phase (V.M. Mishin et al., 1979; Bazarzhapov et al., 1979; McPherron, 1979). The late growth phase sometimes features "pseudobeakups", i.e., localized auroral disturbances with a train of irregular burst pulsations but without the global dipolarization and explosive phase development. Such disturbances may be related to solar wind (SW) sudden impulses.

Unlike the latter, storm sudden commencement (SSC) impulses are followed by storms and substorms (Nishida, 1978). In the substorm theory, a close focus is on the onset of the substorm expansion phase (EP). The EP onset or simply onset, also known as substorm breakup, features the dipolarization, the geomagnetic tail contraction related to the release of the magnetic energy accumulated during the growth phase, and the fast decrease in the polar cap magnetic flux. These processes result in rapidly growing field-aligned currents (FACs) and the intensified auroral activity (V.M. Mishin et al., 2017; Stephens et al., 2019). The EP onset is normally determined by observing the start of the geomagnetic pulsation (Pi2) train at high and mid latitudes, as well as by the auroral intensification (Troitskaya & Guglielmi, 1967; Pudovkin, 1976; Kangas et al., 1998). In addition, broadband burst pulsations or PiBs, with periods T = (0.2–600) s, intensify during the onset. These pulsations involve a short-period part, Pi1B with T = (0.3–40) s, and a long-period part, Pi2-Pi3 with T = (40–600) s (see Table S1 in the Supporting Information). PiBs correlate well with the auroral intensity, *X*-ray bursts, and ionospheric absorption of space radio noise (Troitskaya, 1961; Heacock, 1967; Undiedt et al, 1978; Bösinger et al., 1981; Bösinger & Yakhnin, 1987; Kangas et al., 1998).

During SSCs followed by the storm commencement, burst type pulsations named Psc are generated. They also have a spiky character, the broadband spectrum between 0.2 and 600 s, and the short-period, Psc1,2,3 (0.3–40) s, and long-period, Psc 4,5 (40–600) s, parts (Saito, 1969; Nishida, 1978, see also Table S1). In order to explore the PiB/Psc short-period component, one needs high-frequency resolution data ($\Delta f \geq 10$ Hz, $\Delta t \leq 0.1$ s) whereas most observatories employ magnetometers with a 1-10 s sampling rate. The latter allows studying only longer period Pi2-Pi3 pulsations capable of determining a single EP onset.

However, substorms with double EP onsets are not seldom (Russell, 2000; V.M. Mishin et al., 2001). Those are not resolved in the data of pulsations with periods about and greater than the time interval, τ, between the two onsets. For example, at the start of the 27 August 2001 substorm (Baker et al., 2002; V.M. Mishin et al., 2013, V.M. Mishin et al., 2017), this interval was τ = 2 min. The onsets could be specified using the short period (T < 10 s) component of Pi1B with a shorter duration. It is worth to note concerning the short period component of Pi1B, that the long period (10 –60 s) counterpart has the physical properties similar to Pi2 pulsations (Rae et al., 2011).

In this paper, we analyze the substorm events during the 6 April 2000 and 21 October 2001 superstorms, when the equatorward boundary of the auroral zone was near the city of Irkutsk (CGM: 47.33° Φ, 177.24° Λ). The effects of substorms were recorded both in geomagnetic and optical data. For stormtime substorms with multiple successive intensifications of the *AE* (*AL*) index, the model of an isolated substorm is hardly justified. Rather, quasi-periodic saw-tooth disturbances appear during major storms (Troshichev et al., 2011). The duration of such disturbances may be short, about 15–40 min (V.V. Mishin & Karavaev, 2017). During the 6 April 2000 storm, we also detected a substorm with the growth phase started prior to the SSC at 16:10 UT. The *AE*-index intensifications observed later in the course of the storm are referred to as substorm activations.

2. Database

During the 6 April 2000 and 21 October 2001 storms, we collected geomagnetic data from Mondy (MND; CGM: 47.5° Φ, 177.5° Λ) and Borok (BOX; CGM: 53.9° Φ, 114° Λ) with search-coil magnetometers at a Δf = 10 Hz frequency resolution. During the above events, both stations were located on the night side. In addition, thanks to the Kyoto data center (http://wdc.kugi.kyoto-u.ac.jp), we obtained fluxgate magnetometer data from the low-latitude Kakioka (KAK) station (CGM: 29.25° Φ, 211.7° Λ) with a 1 Hz frequency resolution. Airglow at 557.7 and 630 nm was observed by zenith photometers applying interference oscillating light filters ($\Delta\lambda$ 1/2 ~1–2 nm, V.V. Mishin et al., 2018). The Tory geophysical observatory (TOR) of the ISTP SB RAS is located to the south of Lake Baikal (CGM: 47° Φ, 177° Λ, MLT = UT + 7) about 75 km north-west from Mondy.

We employ the magnetogram inversion technique (MIT) developed at the ISTP SB RAS more than 40 years ago (Bazarzhapov et al., 1979; V.M. Mishin et al., 1979; V.M. Mishin, 1990) and has been upgraded (Lunyshkin & Penskikh, 2019). The MIT method uses the dipolar geomagnetic coordinates: geomagnetic latitude, Φ, and local magnetic time (MLT). Using 1-min data from the network of ground-based magnetometers, we obtained a sequence of Φ-MLT maps of the field-aligned current (FAC) distribution in the ionosphere.

These maps identify the boundaries of the Iijima and Potemra (1978) FAC regions and the values of the magnetic flux, Ψ, from the solar wind through the tail lobes into the magnetosphere (see the definition of Ψ in Section 3). Accordingly, we determine the main onset of the substorm EP at the start of the abrupt decrease of Ψ. The difference between the geomagnetic latitude in the dipole system, Φ, and the latitude Φ_{cor} in the corrected system of geomagnetic coordinates (CGM) used in satellite data is insignificant in the polar cap, but increases equatorward. For Irkutsk, it yields: $\Delta\Phi = \Phi_{cor} - \Phi \approx 48° - 42° \approx 6^0$.

3. Observations of geomagnetic disturbances and airglow

3.1. The 6–7 April 2000 superstorm

The SSC on 6 April 2000 was observed at 16:40 UT. At this time, the solar wind ram pressure (P_d) increased from 1 to 14 nPa, the interplanetary magnetic field (IMF) B_z turned southward to –6 nT, and the IMF *By* component increased to ≈ 20 nT (Figure 1). The *AE*-index increased from 250 nT to 1250 nT; and the D_{st} -index reached its minimum (–287 nT) near 23 UT (V. M. Mishin et al., 2010a; V.V. Mishin et al., 2013; V.V. Mishin & Karavaev, 2017).

On can see in the *H*-component variations at Irkutsk a few bays caused by substorm activations. We will mainly focus on two strongest bays during ~16:40 – 18:10 UT and 19:55 – 20:55 UT indicated in Figure 1 by the red vertical lines. According to the Shue et al, (1998) model, the enhanced SW pressure forced the subsolar magnetopause to $x = 7\ R_E$. Then, the first substorm EP onset occurred, as indicated by the sharply increased *AE* index and, as typical for isolated substorms, by an abnormal increase of the variable part of the magnetic flux, Ψ_1. We denote the difference, Ψ - Ψ_0, between the total polar cap magnetic flux, Ψ, and the pre-substorm value, Ψ_0, as Ψ_1. The total magnetic flux is $\Psi = \int \mathbf{B}(\mathbf{r})\cdot d\mathbf{S}$, where $\mathbf{B}(\mathbf{r})$ is the dipolar geomagnetic field at 115 km and S is the polar cap (R0) area (V.M. Mishin et al., 2001, 2017).

The first EP onset occurred at the end of the growth phase, which started before the SSC (V.M. Mishin et al., 2010a, 2010b). We infer that the polar cap expansion indicated by the increase of Ψ_1 is a direct consequence of the magnetosphere compression. The second EP onset at ~ 16:46 UT (as well as the second substorm activation at ~19:55 UT) is indicated by sharply increasing *AE* and decreasing Ψ_1 due to the magnetotail contraction (dipolarization) after reconnection. The SSC and EP onsets are accompanied by burst pulsations (green arrows in Figure 1).

During 16:40 – 21 UT, MND and BOX recorded several short bursts of broadband irregular Psc/PiB pulsations, whereas TOR recorded bright emissions at 557.7 and 630 nm with intensities of ~100–2500 R after the SSC front arrival (Figure 2). Near 16:40 UT, one can see two double substorm activations. Images from the POLAR satellite (Supplemental Information, Figure S2) also show a weak auroral activation at 16:39 UT and then the real substorm breakup at 16:46 UT in the Northern Hemisphere (MLAT ~40°–90°).

Figure 3 shows the Psc/PiB bursts recorded at the mid-latitude MND and BOX and the low-latitude KAK stations that indicate the double onset of the first substorm activation during the SSC. The first Psc1,2 burst (the first onset) at 16:39:40 UT was recorded during the SSC at periods T>0.4 s at MND and BOX (with a smaller amplitude) and at KAK (T>7 s). The PiB second burst with T>4 s (the second onset) was concurrently recorded by all stations at 16:45:40 UT with the greatest amplitude at MND.

Figure 4 shows isocontours of the downward (upward) FAC density in the Region 1 (R1), Region 2 (R2), and the polar cap – Region 0 (R0). During the SSC, the observatories were 10–15 degrees equatorward of the FAC R2 southern boundary, which descended to the stations in ~5 min and remained there for the EP interval. Although TOR and MND were distant from the westward electrojet (WEJ) maximum, they detected the related intensifications of the green line and burst pulsations.

At 17:10 UT and 18:08 UT, when BOX was near the southern FAC R2+ boundary and MND was ten degrees to the south from the FAC R2– boundary, the *AE* index sharply intensified. This might be consequent to fast variations in the SW pressure and IMF *Bz* (Figure 1). The increase in the *AE* index to 2600 nT was coincident with the increased FACs in the R1, R2 regions to I_{R2-} = 6 MA, I_{R1+} = 8 MA (Figures 1, 4). These two moments were coincident with the intensifications of pulsations at MND and BOX, and 557.7 nm emissions at TOR on the night side (Figures 2, 5).

After 19:00 UT, the observatories were again within the FAC R2 region that caused a strong increase of the airglow intensities (Figure 2). A similar behavior was observed during the 20 November 2003 superstorm (V.V. Mishin et al., 2018). During the second substorm activation interval (19:55–20:55 UT), MND and BOX simultaneously recorded two PiB bursts with T>4 s at 20:00 and 20:13 UT. Their amplitudes were 4 times greater at BOX (Figure 6). At that time, BOX was at the R1/R2 boundary near the WEJ maximum and the focus of the vortex of the upward FAC R2, which is the region of the maximum electron precipitation (Figure 7). Both bursts in the short period range (0.5–10 s) at 19:52 UT and 21:05 UT were detected only at MND.

3.2. The 21 October 2001 superstorm

Figure 8 shows a moderate activity (*AE*~300–400 nT) and slightly enhanced green line emissions (~600 R) before the SSC at 16:48 UT. At the SSC, P_d increased from 2 nP to 20 nP, the southward IMF B_z increased from –5 nT to –21 nT, the IMF B_y turned from +5 nT to –10 nT, and the *AE*-index increased from ~280 nT to 1300 nT. According to the Shue et al. (1998) model, the subsolar magnetopause shifted from $x \approx 10\ R_E$ to $x \approx 5.3\ R_E$. The minimum *SYM-H* (–192 nT) was recorded at 20:25 UT.

The *H*-component variation at IRK, likewise the 6 April 2000 storm, indicated substorm activations (*AE* increases) caused by the amplified SW pressure and the IMF variations at ~16:48 UT, ~18:35 UT, and ~20 UT. At the SSC, the southern boundary of the FAC R2 was far from IRK and BOX. However, after 18:30 UT, and then around 20:00 UT, following the SW pressure increases the boundary moved equatorward of these stations accompanied by two series of PiB pulses and increases in the emission intensities.

The first Psc burst at T>4 s was recorded at MND at 16:48 UT and also during the first substorm activation (Figures 8 and 9). During the substorm activations after the SSC, there occurred two PiB bursts at 18:18:04 and 18:30:26 UT, and then three PiB/PiC bursts after 20 UT with T>0.4 s and intensified green and red line emissions (Figure 9). At that time, MND and TOR were inside the FAC R2 region.

4. Discussion

Section 3 describes several substorm activations accompanied by broadband PiB/PiC bursts and airglow in the nightside mid-latitude atmosphere during the 6 April 2000 and 21 October 2001 events. Further, we discuss only the April 6, 2000 superstorm because the second event is very similar.

4.1. Short- vs. long-period pulsations

First, we would like to justify the advantage of the short period and wavelength Pi1B pulsations for timing EP onsets. These pulsations vanish faster in space and time than their longer period and wavelength counterparts. Obviously, to resolve Pi1Bs, one needs records of a ≥10 Hz frequency resolution rarely available at geomagnetic observatories. Precisely, the high time resolution magnetic data from the MND and BOX stations allowed us to determine the EP double onset at t_1 = 16:39:40 UT and t_2 = 16:45:40 UT ($\tau = t_2 - t_1 = 6$ min) during the 6 April 2000 superstorm. The same onsets (t_1, t_2) are revealed from the dynamic spectrum of the geomagnetic field oscillations at periods in the range of 8–40 s obtained at the KAK station (Figure 3).

We note that a small duration of the Pi1B train (<1 min) makes possible not only tracing the EP onsets but also picking out the double onsets. This is practically impossible with the PiB's long-period part (Pi2/Pi3 pulsations). Namely, when their period (T_{long}) is close to the interval, τ, between the onsets, one pulsation train turns continuously into another. The latter is evident in the dynamic spectra with 40–60 s periods from MND, BOX, and KAK (Figure 3). It is relevant to note that V.V. Mishin et al. (2003, Figures 5 and 6) found from high resolution oscillograms of pulsations excited by SW pulses that the first pulsation dies outs prior to the start of the second one only if the interval between SW pulses is sufficiently large: $\tau \gg T_{long}$.

Note that Cheng et al. (2018) attempted to determine the double substorm onset by the decrease in the Pi2 period. They attributed the change to the tail shortening during the EP onset. In fact, however, such a change of the Pi2/Pi3 period is dubious as there were only two periods between the studied onsets, i.e., $\tau = 2T_{long}$. Such period decrease is characteristic of only a special type of short period pulsations called IPDP (Kangas et al., 1998).

We will illustrate a more adequate determination of the duration, $\Delta\tau$, of Psc1,2/PiB bursts, which depends on the frequency resolution, Δf, using the 16:40 UT event on 6 April 2000 as an example. Figure 10 shows the Psc1 dynamic spectra obtained at MND with the sampling rate of 10 Hz and at KAK with 1 s data. It is seen that the burst lasted for $\Delta\tau \leq 20$ s at MND, which is in a good agreement with an estimate $\Delta\tau$ =15 s from a detailed study by Parkhomov et al. (2010). At KAK the burst lasted for $\Delta\tau$ =2–3 min, i.e., $\Delta\tau$ decreased with the increase of Δf . Clearly, timing the isolated substorm EP onsets and substorm activations during storms is more accurate with high-frequency sampling rates (Δf >10 Hz).

As an example, let us note the CARISMA network data. Particularly, Rae et al. (2009, 2011) using wavelet analysis of the CARISMA data with a 1 s resolution obtained a number of important results on the relationship between the most equatorward auroral arc and the time of the expansion onset determined from Pi1 pulsations. Presently, the network employs induction magnetometers with a 20 Hz sampling rate. This will certainly improve the accuracy of determining the time of the EP onset in pulsations and auroras. The new capability of the CARISMA network may also help to clarify the features of PIBs in the short period range discussed below.

4.2. Generation mechanism

We now turn to discuss possible generation mechanisms of the observed pulsations and optical emissions. The Psc generation is usually attributed to the arrival of the interplanetary shock front (Nishida, 1978). In the studied event, the SW plasma density (pressure) increased ahead of the front twice at 16:31:20 UT and at 16:35:16 UT (V.V. Mishin et al., 2013, Figure 8). That occurred during the substorm growth phase initiated by the IMF turning southward about 20 min prior to the SSC (Figure 1). The P_d pulses caused weak auroral emissions at 16:33:43 UT that slightly intensified during the first onset at 16:39:51 UT (Figure S2). As shown earlier by V.V. Mishin et al. (2013), the SW pressure enhancements resulted in MHD disturbances that propagated during 16:36–16:40 UT from the dayside to the nightside. After that, MHD waves coming in the opposite direction emerged from a possible nighttime substorm source during 16:41–16:44 UT.

The burst of pulsations related to the SSC results from the impact of the interplanetary shock front on the magnetopause. Pulsations appear at mid- and low-latitude stations in accordance with the source's global character (Parkhomov et al., 2017). According to Mishin et al. (2013), we attribute the first burst of pulsations at MND and BOX to the Psc type caused by the daytime source. At the same time (Figure 3), the effect of the substorm development is indicated by the fact that the pulsations at MND (premidnight) were more enhanced than at BOX (duskside).

We ascribe the other bursts to the PiB type, though three of them (at 16:46 UT, 17:10 UT, and 18:08 UT) occurred during the period of rapid variations of the SW pressure. Nonetheless, these bursts were coincident with sharp intensifications of the *AE* index on the top of its greatly elevated mean level. The bursts' location in the near midnight region is natural for the development of the substorm current wedge (V.M. Mishin et al., 2010 a, b; 2011). What is more, the bursts after the SSC were coincident with prompt changes of the near-midnight upward R1 and R2 FACs that maximized at the center of R2– vortices near the boundary of the R1+ zone. Here, the maximum of the westward electrojet (WEJ) is located, which corresponds to energetic electron precipitation and auroras (e.g. V.M. Mishin, 1990; Korth et al., 2014, Carter et al., 2016). It is also relevant to note that the Pi1B maximum intensity correlates with the WEJ maximum (Parkhomov & Rakhmatulin, 1975; Despirak, et al., 2020).

At the time of the second (main) substorm EP onset at 16:46 UT, the *AE* and *AL* indices, FACs, and optical emissions intensified. However, there was only slight increase of pulsations at BOX, most likely because the station was too far from the R2–/R1+ and auroral oval boundaries (Figures 1 – 5 and Figures S1, S2). The next two PiBs were also detected during pressure pulses and strong geomagnetic activity (AE = 2600 nT and FACs R1.2 = 6-8 MA). The Pi1B amplitude at MND at 17:10 UT was much larger than at BOX, which was farther than MND from the R1– boundary (Figure 5).

At 18:08 UT, when BOX was close to the R2+/R1– boundary, the Pi1B amplitude increased by more than an order of magnitude relative to that at 17:10 UT (Figures 4 and 5). This bears witness of the dependence of the PiB magnitude on the distance from the upward FAC regions. This conjecture agrees with the data of the second substorm activation. Particularly, when the R2– boundary approached MND, the amplitude of pulsations increased by 1.5 times still remaining weaker than at BOX by a factor of two because of the greater distance to the maximum of the upward R2– FAC.

At about 20 UT, both stations were located near or inside Region 2–, but BOX was at the boundary R2–/R1 +, i.e., much closer to the upward FAC maximum. Accordingly, enhanced T>4 s pulsations observed at BOX were 4 times greater than at MND. At the same time, a sharp attenuation was seen in the range T<4 s (Figures 6 and 7). In addition, the maximum airglow intensity was observed from TOR during 19–20 UT. The latter, together with the amplification of the upward FAC, indicates that the electron precipitation was moving toward MND and TOR.

Therefore, we conclude that PiB pulsations were excited by rapid increases in the substorm FACs' intensity indicated by the WEJ and *AE* index (mainly determined by *AL*, see Figure S1). The amplitude of the core spectrum of pulsations increased when the upward R2– FAC boundary on the nightside approached the stations. However, at the R2–/R1+ border, near the focus of FAC R2– and hence electron precipitation, the amplitude of the pulsations in the range T<4 s significantly decreased. In particular, near local midnight (at 00:10 MLT and 01:08 MLT), their intensity at MND dropped almost threefold (Figure 3). When BOX approached midnight (23 MLT), the Pi1B at 0.2–4 s also weakened, barely exceeding the noise level. However, the longer period part of pulsations (> 4 s) increased at that time.

We assume that this behavior is related to the change of the conductivity in the premidnight (superstorm auroral/subauroral) ionosphere near Irkutsk. Indeed, around 20 UT the BOX station was near the R1/R2 boundary, slightly northward of the maximum of the upward R2– FAC, that is, the maximum of energetic electron precipitation (e.g., V.M. Mishin, 1990; Korth et al., 2014; Carter et al., 2016). This agrees well with the intensification of optical emissions from TOR during 19–20 UT. Surely, energetic electrons increase the E-region conductivity and hence the electromagnetic impedance. As a rule, this results in weakening of penetration of the short period pulsations into the lower ionosphere (Lyatsky & Maltsev., 1983; Klibanova et al., 2008).

In other words, the impermeability of the lower wall of the ionospheric Alfvén resonator (IAR, see shortly) increases. For longer period, T>4 s, oscillations with wavelengths greater than the height of the E layer ($\lambda > h_E \sim 120$ km) such a screening effect is unimportant. Therefore, the oscillations with T>4 s amplified when the FAC R2– and the WEJ maximum approached the BOX station. The presence of the short period pulsations at MND at that time was because the station, most likely, remained in the subauroral region equatorward of the electron precipitation where the conductivity was low.

From the above analysis, we conclude that the impact of the interplanetary shock front was responsible for bursts of Psc pulsations observed near the SSC. On the other hand, Nishida (1978) and Parkhomov et al. (2017) attributed Psc to the development of ion cyclotron instability caused by the transverse anisotropy on the outer L shells (L> 6) where the proton gyrofrequency, $\omega_{Bp} = eB/m_p \approx 3 \cdot 10^3 / L^3$ (s^{-1}), falls into the range of short-period pulsations Psc1,2. The data from the LANL 94 satellite, which was at the longitude of Irkutsk (Figure S3), give evidence in favor of this mechanism at the beginning of the 6 April 2000 storm. Prior to the storm, the transverse anisotropy, characteristic of the trapped plasma, practically disappears after SSC.

One of the main tasks of the Pi1B/Psc theory is to explain a continuous broadband spectrum with the resonant structure. The latter is characteristic of the spectrum of the IAR model (Polyakov & Rapoport, 1981). The lower wall of the resonator is due to the maximum conductivity in the E layer. The upper wall is formed at height h ~ 3000 km by the inflection of the Alfven velocity profile related to the decrease of the plasma density. A typical theoretical spectrum features diffuse resonance maxima on the top of enhanced quasi-continuous 0.1 Hz – 2 Hz noise with a noticeable decrease in amplitude at frequencies greater than 0.5 Hz (Lysak, 1988). Therefore, it is reasonable to suggest that the continuous spectrum of the Pi1B and Psc1,2 pulsations is associated with their passage through the IAR (cf. Lysak, 1988; Parkhomov et al., 2017).

Further, recall the similarity of the observed pulsations, such as a sequence of a few oscillations containing the periodic resonant structure and rapidly decaying just after they emerged. This behavior suggests that they resulted from a pulsed electromagnetic impact on the IAR similar to a lightning discharge, seismic oscillations, solar wind pressure pulses (Dovbnya et al., 2014) or even injection of ion beams into the IAR region for a few seconds (Volokitin & Drozdov, 1993). Lysak (1988) surmised that PiBs may be excited by a strong pulsed change of the field - aligned currents. This is consistent with the observations of PiBs during auroral current enhancements (Untiedt et al., 1978; Opgenoorth et al., 1980).

This is also consistent with our observations of Pi1B bursts after fast increases in the *AE* index, magnetic flux, Ψ, and corresponding FACs - the characteristic feature of the EP onset according to MIT (V.M. Mishin, 1990). Recall, for example, the second EP onset at 16:46 UT with the sharp increase in the *AE* index and fast equatorward motion to mid latitudes of the FAC regions with the several-fold increase in the FAC intensity (Figures 1, 4).

A final remark is in order regarding the ionospheric feedback instability (IFI). A large number of works invoke the IFI to explain processes during the substorm EP onset. The IFI develops in the presence of a sufficiently large convection electric field, E_c, due to deceleration of the plasma convection and formation of a strong vertical shear in the convection flow in the ionosphere (Trakhtengertz & Feldstein, 1981, 1991; Lysak, 1988; Lysak, 1991). Precipitation of energetic electrons and the presence of depleted conductivity frequently occurring in the FAC R2– are favorable factors for the IFI development (Streltsov & Mishin, 2018). However, in the events studied in this paper, we did not find in situ data clearly supporting the IFI development near the MND and BOX observatories.

5. Conclusion

The main goal of this work is to show that using short-period burst pulsations allows determining the substorm expansion onsets more accurately than using conventional Pi2 pulsations. In addition, this method is well suited for picking out double onsets and stormtime substorm activations inaccessible for Pi2. In particular, we have shown that

1. Intensifications of mid-latitude broadband geomagnetic pulsations (Psc/PiBs) and airglow during two strong magnetic storms mark the substorm expansion onsets or the onset of short substorm activations.

2. Detecting the Psc/PiB short period part (Psc1,2/Pi1B) makes possible to identify a single onset and to separate double substorm onsets, as well as series of onsets of short substorm activations during storms, with the accuracy better than 0.5 min.

3. Burst pulsations with a broadband spectrum containing the periodic resonant structure are excited in the ionospheric Alfvén resonator impacted by a pulsed change of the field-aligned currents in the substorm current wedge circuit.

4. We attribute the near-midnight minimum of pulsations within the 0.2–4 sec periods to the weakening of their penetration due to enhanced precipitation of energetic electrons

Acknowledgements

B.T. is supported by the grant ShUSS-2017/65 from the Ministry of Education, Science and Sport (Mongolia).The study was performed with budgetary funding from Basic Research program II.16. and partially supported by the Russian Foundation for Basic Research under Grants No. 18-05-00437 and 19-05-00665. The authors thank Yu.V. Penskikh for calculating FAC regions boundaries for the 2001 storm, A.S. Potapov and A.R. Rakhmatulin for the 10-Hz geomagnetic data from the MND and BOX, and A.V. Mikhalev for the TOR optical data. Data is available through (Afraimovich et al., 2002) and (Parkhomov et al., 2018). We are also grateful to all of the above colleagues for fruitful discussions.

For the ground magnetometer 1-min data, we are thankful to PIs of the CARISMA, INTERMAGNET, GIMA, MACCS and IMAGE international projects and of magnetic networks in Arctic and the Antarctic (Arctic and Antarctic Research Institute, and DMI), and individual Russian and Japan magnetic observatories for providing magnetic data used in this study. Available geomagnetic data are obtained directly from http://www.intermagnet.org/data-donnee/download-eng.php (INTERMAGNET), http://space.fmi.fi/image/ (IMAGE), http://space.augsburg.edu/maccs/request.jsp (MACCS), https://www.asf.alaska.edu/magnetometer (GIMA), and http://www.carisma.ca (CARISMA). The SW key parameters and optical observations of auroras from POLAR were obtained through the NASA Space Science Data Coordinated Archive (http://cdaweb.gsfc.nasa.gov/). The *AE* index was obtained through the SuperMAG website (http://supermag.jhuapl.edu).

References

Akasofu, S. I. (1964), The development of the auroral substorm, *Planet. Space Sci., 12*, 273.

Afraimovich E.L., Ya.F. Ashkaliev, V.M. Aushev, A.B. Beletsky, V.V. Vodyannikov, L.A. Leonovich, O.S. Lesyuta, Yu.V. Lipko, A.V. Mikhalev, A.F. Yakovets (2002), Simultaneous radio and optical observations of the mid-latitude atmospheric response to a major geomagnetic storm of 6–8 April 2000, Journal of Atmospheric and Solar-Terrestrial Physics 64, 1943– 1955. https://doi.org/10.1016/S1364-6826(02)00217-1

Baker, D. N., W. K. Peterson, S. Eriksson, X. Li, J. B. Blake, J. L. Burch, P. W. Daly, M. W. Dunlop, A. Korth, E. Donovan, R. Friedel, T. A. Fritz, H. U. Frey, S. B. Mende, J. Roeder & H. J. Singer (2002), Timing of magnetic reconnection initiation during a global magnetospheric substorm onset, *Geophys. Res. Lett.*, *29*(24), 2190. https://doi:10.1029/2002GL015539.

Bazarzhapov, A. D., M. I. Matveev, V. M. Mishin (1979), Geomagnetic Variations & Storms. *Nauka Publ*, (In Russian).

Bösinger, T., K. Alanko, J. Kangas, H. Opgenoorth, *W. Baumjohann (1981), Correlations between *PiB* type magnetic micropulsations, auroras and equivalent current structures during two isolated substorms, *Journal of Atmosphenc and Terrestrial Physics*, *43*(9), 933-945. https://doi.org/10.1016/0021-9169(81)90085-4

Bösinger, T., A. & G. Yahnin (1987), Pi1B type magnetic pulsations as a high time resolution monitor of substorm development, *Annales Geophysicae, 5 A*, 231–238.

Brunelli, B. Y., A. A. Namgaladze (1988), Physics of Ionosphere. *Nauka*, *Moscow*, 528, (In Russian)

Carter, J. A., S. E. Milan, J. C. Coxon, M. T. Walach, & B. J. Anderson (2016), Average field-aligned current configuration parameterised by solar wind conditions, *J. Geophys. Res. Space Physics*, *121*(2), 1294-1307. https://doi:10.1002/2015ja021567.

Cheng, C.-C., Russell, C. T., Mann, I. R., E. Donovan, W. Baumjohann (2018), Characteristic study of double substorm onsets in response to IMF variations, *Ann. Geophys., Discuss., 116*. https://doi.org/10.5194/angeo-2018-116.

Despirak, I. V., T. V. Kozelova, B. V. Kozelov, A. A. Lubchich (2020), Westward propagation of substorm by THEMIS and ground-based observations, *Journal of Atmospheric and Solar–Terrestrial Physics, 206*. https://doi.org/10.1016/j.jastp.2020.105325

Dovbnya, B. V., A. S. Potapov, A. V. Guglielmi, R. A. Rakhmatulin (2014), On the impact of MHD resonators on the geomagnetic pulsations // *Geophysical Journal, 36* (6), 143–152. https://doi.org/10.24028/gzh.0203-3100.v36i6.2014.111053

Heacock, R. R. (1967), Two subtypes of Pi micropulsations. *J. Geophys. Res. 72*(15), 3905–3917. https://doi:10.1029/JZ072i015p03905.

Iijima, T., & T. A. Potemra (1978), Large-scale characteristics of field-aligned currents associated with substorms, *J. Geophys. Res*, *83*(A2), 599–615. https://doi:10.1029/JA083iA02p00599.

Kangas, J. (1998), Morphology and physics of short-period magnetic pulsations, *Space Sci. Rev., 83,* 435–512.

Klibanova, Yu. Yu., Mishin, V. V., B. Tsegmed (2008), Short-period geomagnetic pulsations and optical glows in the mid-latitude atmosphere during superstorms, *Sol.-Terr. Phys., 2* (12), 334–335 (in Russian)

Klibanova, Yu. Yu., V. V. Mishin, A. V. Mikhalev, B. Tsegmed, Yu. A. Karavaev, M.A. Kurikalova (2019), Dynamics for geomagnetic pulsations, field aligned currents, and airglow at midlatitudes within substorm activations during superstorms, *Geodynamics & Tectonophysics*, *10*(3), 673–685. https://doi:10.5800/GT20191030434.

Korth, H., Y. Zhang, B. J. Anderson, T. Sotirelis, & C. L. Waters (2014), Statistical relationship between large-scale upward field-aligned currents and electron precipitation, *J. Geophys. Res. Space Physics, 119*(8), 6715-6731. https://doi:10.1002/2014ja019961.

Lunyushkin S.B., Yu. Penskikh (2019), Diagnostics of auroral oval boundaries on the basis of the magnetogram inversion technique, *Sol.-Terr. Phys.*, *5*(2), 88–100. https://doi:10.12737/stp-52201913.

Lyatsky, W. B., Ya. P. Maltsev (1983), The magnetosphere-ionosphere interaction, *Results of researches on the international geophysical project*, Nauka, Moscow (in Russian).

Lysak, R. L. (1988), Theory of auraoral PiB pulsation spectra. *Journal of Geophysical Research, 93*(A6), 5942. https://doi.org/10.1029/JA093iA06p05942

Lysak, R. L. (1991), Feedback instability of the ionospheric resonant cavity. *Journal of Geophysical Research*, *96*(A2), 1553-1568. https://doi:10.1029/90JA02154

McPherron, R. L. (1979), Magnetospheric Substorms, *Rev. Geophys. Space Phys.*, *17*, 657–681.

Mikhalev, A.V. (2013), Midlatitude airglows in East Siberia in 1991–2012, *Sol.-Terr. Phys.*, *24*, 78–83 (in Russian)

Mishin V. M. (1990), The magnetogram inversion technique and some applications, *Space Science Reviews*, *53*(1-2), 83-163.

Mishin, V. M., A. D. Bazarzhapov, G.B. Shpynev (1979), Electric Fields and Currents in the Earth's Magnetosphere, in *Dynamics of the Magnetosphere*, edited by S. I. Akasofu, pp. 249–268, Springer, Netherlands, https://doi:10.1007/978-94-009-9519-2_12.

Mishin, V. M., M. A. Kurikalova, & M. Förster (2010a), Electric circuits and their generators in the earth's magnetosphere: The concept of electric circuits as applied to the first phase of the April 6, 2000 superstorm, *Geomagnetism and Aeronomy*, *50*(8), 978-987. https://doi:10.1134/s0016793210080086.

Mishin, V. M., M. A. Kurikalova, & M.V. Tolochko (2010b), Superstorm of 06.04.2000: effects of strong dynamic shocks, *Solar-Terrestrial Physics*, *15*, 96-106 (in Russian).

Mishin, V. M., M. Förster, M. A. Kurikalova, & V. V. Mishin (2011), The generator system of field-aligned currents during the April 06, 2000, superstorm, *Advances in Space Research*, *48*(7), 1172-1183. https://doi.org/10.1016/j.asr.2011.05.029.

Mishin, V. M., T. Saifudinova, A. Bazarzhapov, C.T. Russell, W. Baumjohann, R. Nakamura & M. Kubyshkina (2001), Two distinct substorm onsets, *Journal of Geophysical Research: Space Physics*, *106*(A7), 13105-13118. https://doi:10.1029/2000ja900152.

Mishin, V. M., V. V. Mishin, S. B. Lunyushkin, J. Y. Wang & A.V. Moiseev (2017), 27 August 2001 substorm: Preonset phenomena, two main onsets, field-aligned current systems, and plasma flow channels in the ionosphere and in the magnetosphere, *J. Geophys. Res: Space Physics*, *122*(A5) 4988–5007. https://doi:10.1002/2017JA023915.

Mishin, V. M., Z. Pu, V. V. Mishin, & S. B. Lunyushkin (2013), Short-circuit in the magnetosphere-ionosphere electric circuit, *Geomagnetism and Aeronomy*, *53*(6), 809-811. https://doi:10.1134/s001679321306008x.

Mishin, V. V., A. Yu. Pashinin, V. A. Parkhomov (2003), Geomagnetic pulsations caused by the magnetopause oscillations (comparison of spacecraft and geomagnetic observations), *Advances in. Space Research*, *31*(5), 1177–1182. https://doi:10.1016/S0273-1177(02)00932-8.

Mishin, V. V., S. B. Lunyushkin, A. V. Mikhalev, Yu. Yu. Klibanova, B. Tsegmed, Yu. A. Karavaev, A. V. Tashchilin, L. A. Leonovich, Yu. V. Penskikh (2018), Extreme geomagnetic and optical disturbances over Irkutsk during the 2003 November 20 superstorm, *Journal of Atmospheric and Solar-Terrestrial Physics*, *181*, 68–78. https://doi.org/10.1016/j.jastp.2018.10.013.

Mishin, V. V., Yu. A. Karavaev (2017). Saturation of the magnetosphere during superstorms: new results from the magnetogram inversion technique, *Sol.-Terr. Phys.*, *3*(3), 28–36. https://doi:10.12737/stp-33201704.

Mishin, V. V., Yu. Yu. Klibanova. B. Tsegmed (2013), Solar wind inhomogeneity front inclination effect on properties of front-caused long-period geomagnetic pulsations, *Cos. Res., 51*(2), 96–107. https://doi:10.7868/S0023420613020027.

Nishida, A. (1978), Geomagnetic Diagnosis of the Magnetosphere, *New York; Heidelberg; Berlin: Springer-Verlag*, 256.

Opgenoorth, H. J., R. J. Pellinen, H. Maurer, F. Kueppers, W. J. Heikkila, K. U. Kaila, & P. Tanskanen (1980), Ground-based observations of an onset of localized field-aligned currents during auroral breakup around magnetic midnight, *J. Geophys., 48*, 101.

Parkhomov, V. A., G. N. Zastenker., M.O. Riazantseva, B. Tsegmed, T. A. Popova (2010), Bursts of geomagnetic pulsations in the frequency range 0.2–5 Hz excited by large changes of the solar wind pressure, *Cosmic Research, 48*(1), 86–100. https://doi:10.1134/S0010952510010077.

Parkhomov, V. A., N. L. Borodkova, A. G. Yahnin, B. V. Kozelov, A. V. Suvorova, B.V. Dovbnya, A. Y. Pashinin (2017), Global impulse burst of geomagnetic pulsations in the frequency range of 0.2–5 Hz as a precursor of the sudden commencement of st. patrick's day 2015 geomagnetic storm, C*osmic Research, 55*(5), 307–317. https://doi:10.1134/S0010952517050070.

Parkhomov, V. A., R. A. Rakhmatulin (1975), Localization of Pi1B source, *Issledovaniya po geomagnetizmu, aeronomii i fizike Solntsa [Research on Geomagnetism, Aeronomy and Solar Physics], 36*, 132–138 (in Russian).

Polyakov, S. V. & V. O. Rapoport (1981), Ionospheric Alfven resonator, *Geomagn. Aeron., 21*, 816.

Pudovkin, M. I., O. M. Raspopov, N. G. Kleimenova (1976). Disturbances of Electromagnetic Field of the Earth. Part 2. Short-period oscillations of the geomagnetic field, *Leningrad State University Publishing House, Leningrad*, 271, (in Russian).

Rae, I. J, I. R. Mann, K. R. Murphy, D. K. Milling, A. Parent, V. Angelopoulos, H. U. Frey, A. Kale, C. E. J. Watt, S. B. Mende, C. T. Russell (2009). Timing and localization of ionospheric signatures associated with substorm expansion phase onset *J. Geophys. Res*, *114*, A00C09. https://doi:10.1029/2008JA013559.

Rae, I. J., K. R. Murphy, C. E. J. Watt, & II. R. Man (2011), On the nature of ULF wave power during nightside auroral activations and substorms: 2. Temporal evolution. *J. Geophys. Res., 116*, A00I22. https://doi:10.1029/2010JA015762.

Rassoul, H. K., R. P. Rohrbaugh, B. A. Tinsley & D. W. Slater (1993), Spectrometric and photometric observations of low-latitude aurorae, *J. Geophys. Res. 98* (A5), 7695–7709.

Russell, C. T. (2000), How northward turnings of the IMF can lead to substorm expansion onsets, *Geophys. Res. Lett.*, *27*(20), 3257–3259. https://doi:10.1029/2000gl011910.

Saito, T. (1969), Geomagnetic pulsations, *Space Science Reviews 10(3)*, 319-412.

Shue, J.-H., P. Song, C. T. Russell, J. T. Steinberg, J. K. Chao, G. Zastenker, O. L. Vaisberg, S. Kokubun, H. Singe., T. R. Detman & H. Kawano (1998), Magnetopause location under extreme solar wind conditions, *J. Geophys. Res.*, *103*(A8), 17.691–17.700.

Stephens, G. K., M. I. Sitnov, H. Korth, N. A. Tsyganenko, S. Ohtani, M. Gkioulidou, & A. Y. Ukhorskiy (2019), Global Empirical Picture of Magnetospheric Substorms Inferred From Multimission Magnetometer Data, *J. Geophys. Res: Space Physics*, *124*(2), 1085–1110. https://doi:10.1029/2018ja025843.

Streltsov, A. V. & E. V. Mishin (2018), On the Existence of Ionospheric Feedback Instability in the Earth's Magnetosphere-Ionosphere System, *Journal of Geophysical Research: Space Physics 123*(11), 8951-8957. https://doi:10.1029/2018JA025942.

Tinsley, B. A., R. Rohrbaugh, H. Rassoul, Y. Sahai, N. R. Teixeira, D. Slater (1986), Low-latitude aurorae and storm time current systems, *J. Geophys. Res: Space Physics*, *91*(A10), 11257–11269. https://doi.org/10.1029/ JA091iA10p11257.

Trakhtengerts, V. Yu. & A. Ya. Feldstein (1981), Influence of Alfven velocity inhomogeneous profile on magnetospheric convection stratification, *Geomagn. Aeron.*, *21*, 951 (in Russian).

Trakhtengerts, V. Yu. & A. Ya. Feldstein (1991), Turbulent Alfven boundary layer in the polar ionosphere 1. Excitation conditions and energetics. *J. Geophys. Res.*, *96*(A11), 19,363-19,374.

Troitskaya, V. A. & A. V. Guglielmi (1967), Geomagnetic Micropulsations and Diagnostics of the Magnetosphere, *Space Sci. Rev. 7*(5-6), 689–768.

Troitskaya, V. A.(1961), Pulsation of the Earth's electromagnetic field with periods of 1 to 15 seconds and their connection with phenomena in the high atmosphere, *J. Geophys. Res.*, *66*(1), 5–18. https://doi.org/10.1029/JZ066i001p00005.

Troshichev, O., P. Stauning, K. Liou, G. Reeves (2011), Saw-tooth substorms: Inconsistency of repetitive bay-like magnetic disturbances with behavior of aurora, *Adv. Space Res.*, *47*, 702–709.

Untiedt, J., R. Pellinen, F. Kueppers, H. J. Opgenoorth, W. D. Pelster, W. Baumjohann, H. Ranta, J. Kangas, P. Czechowsky, & W. J. Heikkila (1978), Observations of the initial development of an auroral and magnetic substorm at magnetic midnight, *J. Geophys.*, *45*, 41.

Volokitin, A. S., A. B. Drozdov (1993), Excitation of an Alfven resonator during the injection of an ion beam in the ionosphere, *Geomagnetizm i Aeronomiya* (ISSN 0016-7940), *33*(3), 50-58.

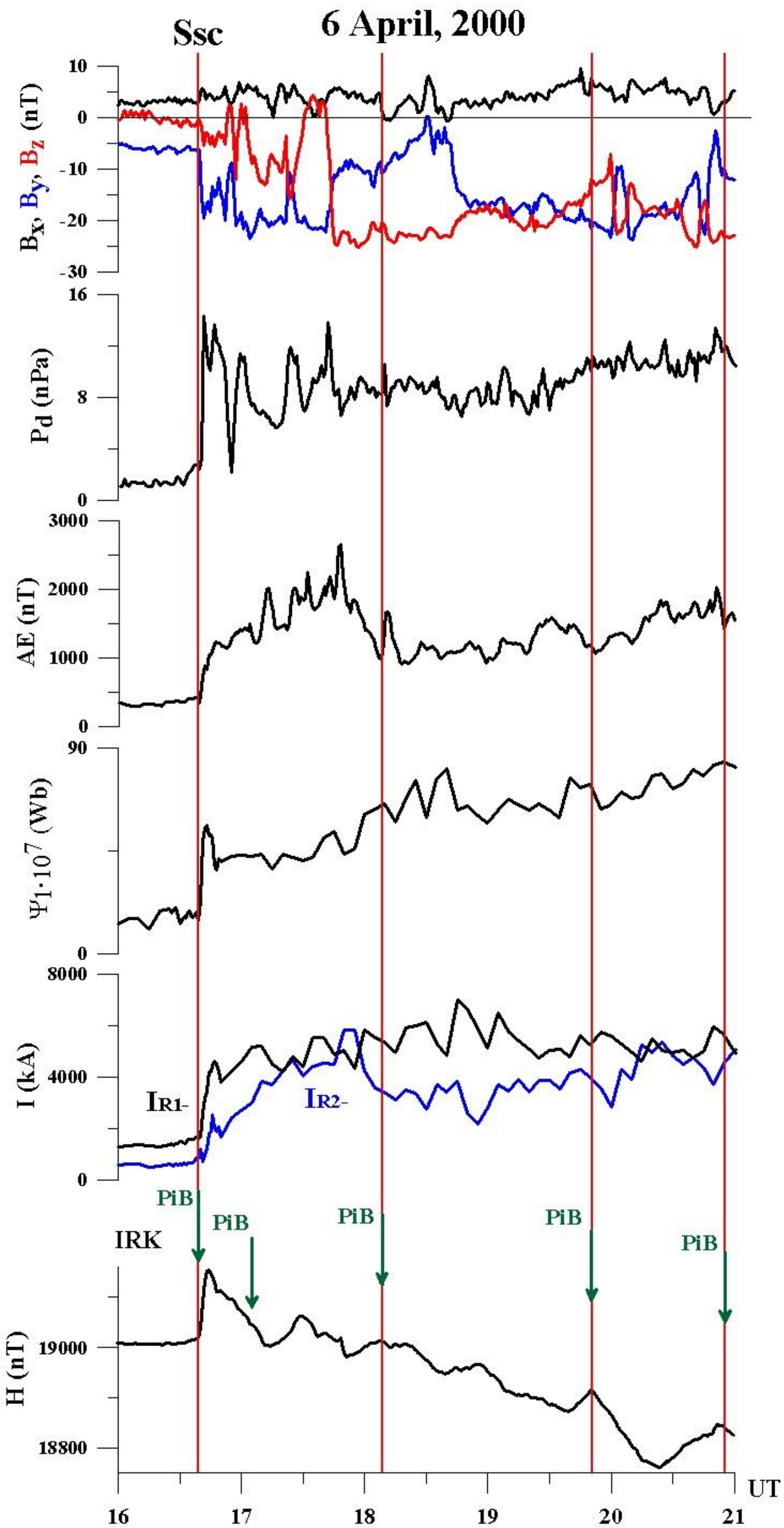

Figure 1. The 6-7 Apr 2000 superstorm. From top to bottom: Variations in the IMF components, solar wind ram pressure (P_d), *AE*-index, magnetic flux through the polar cap, Ψ_1, FAC intensities in the R1–, R2– regions, and the *H*-component at IRK. Red lines show the boundaries of two intervals of substorm activations.

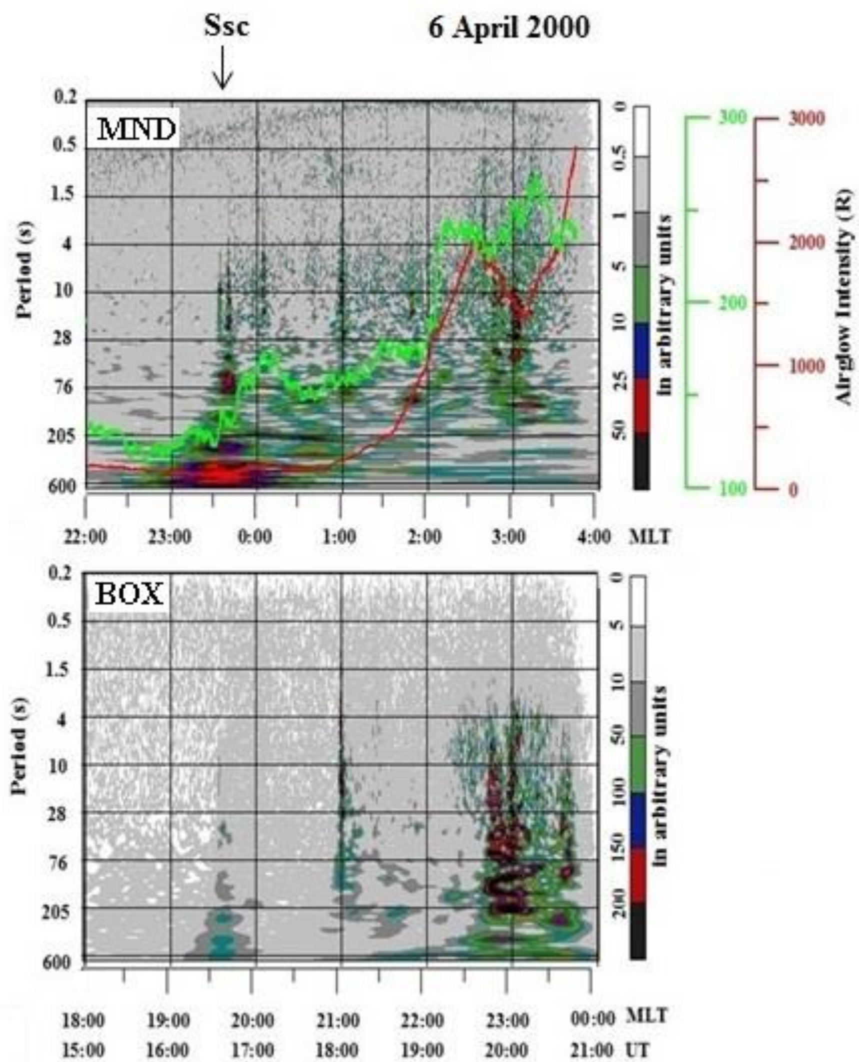

Figure 2. Dynamic spectra of geomagnetic pulsations from (top) MND and (bottom) BOX during the 6-7 Apr 2000 superstorm: The amplitude variation in arbitrary units as a function of the period and universal time (UT) or magnetic local time (MLT). The green (red) line shows the intensity in Rayleigh of the 557.7 nm (630.0 nm) emission from TOR (intensity scales are on right, top panel).

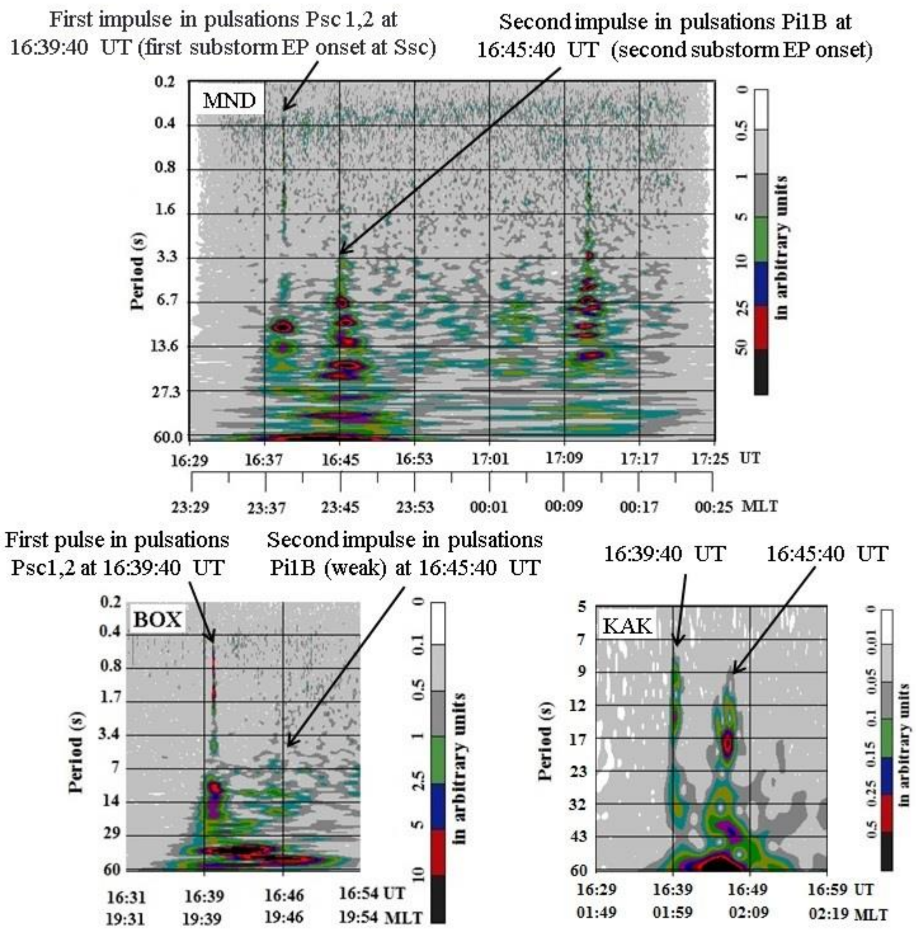

Figure 3. Dynamic spectra of the Psc/PiB geomagnetic pulsations from the MND (CGM: 47.5° Φ, 177.5° Λ), BOX (CGM: 53.9° Φ, 114° Λ), and KAK (CGM: 29.25° Φ, 211.7° Λ) during the 6 April 2000 first substorm activation.

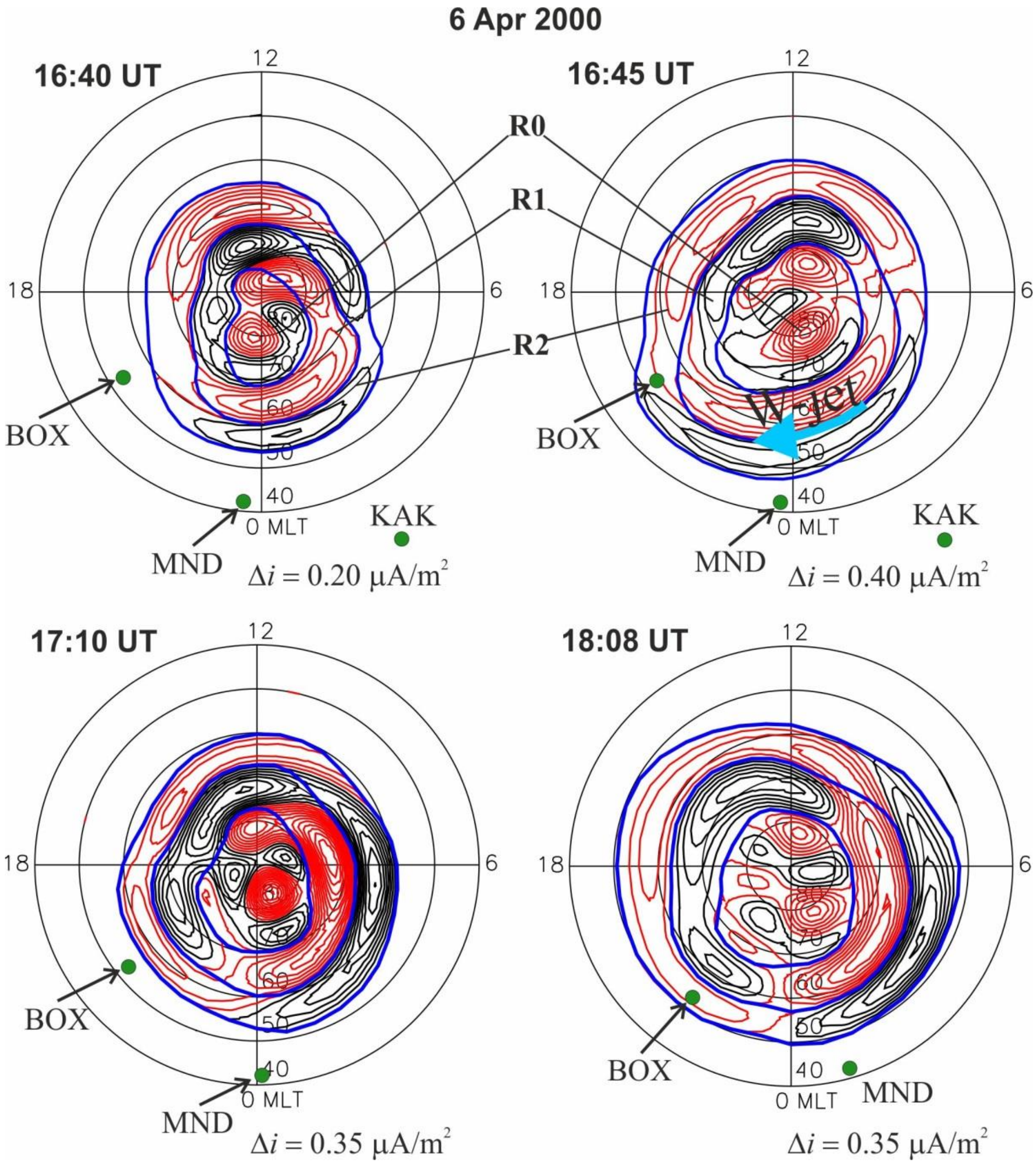

Figure 4. Magnetogram Inversion Technique MLAT-MLT maps of the FAC density distribution at (top panel) 16:40 and 16:45 UT (double EP onset at the start of the 6 April 2000 superstorm and first substorm activation) and (bottom) at 17:10 and 18:08 UT. Blue thick lines show the boundaries of the FAC R1, R2, and of the polar cap, R0. Red (black) isolines are isocontours of the downward (upward) FAC density. Green bold dots show the locations of the observatories.

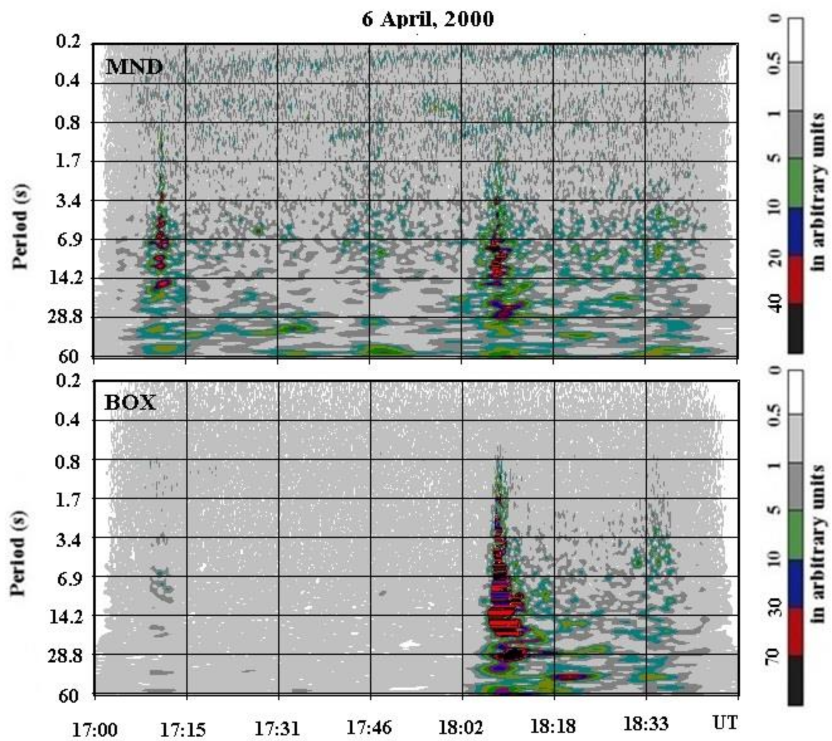

Figure 5. Dynamic spectra of geomagnetic pulsations from the MND and BOX during the 6-7 Apr 2000 superstorm. Shown are: the amplitude variations depending on the period (ordinate), universal time (UT). The relative amplitude values feature a color scale in relative units.

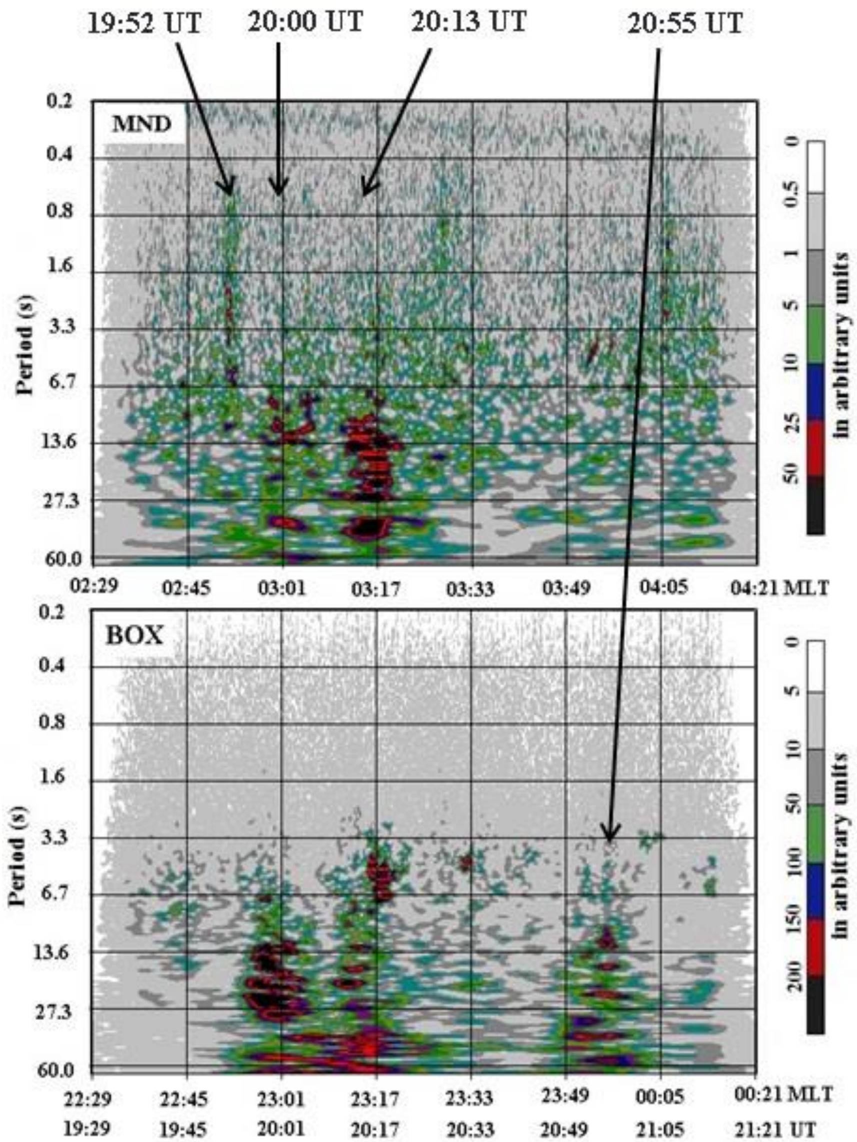

Figure 6. PiB dynamic spectra from MND (CGM: 47.5° Φ, 177.5° Λ) and BOX (CGM: 53.9° Φ, 114° Λ) during the substorm second activation.

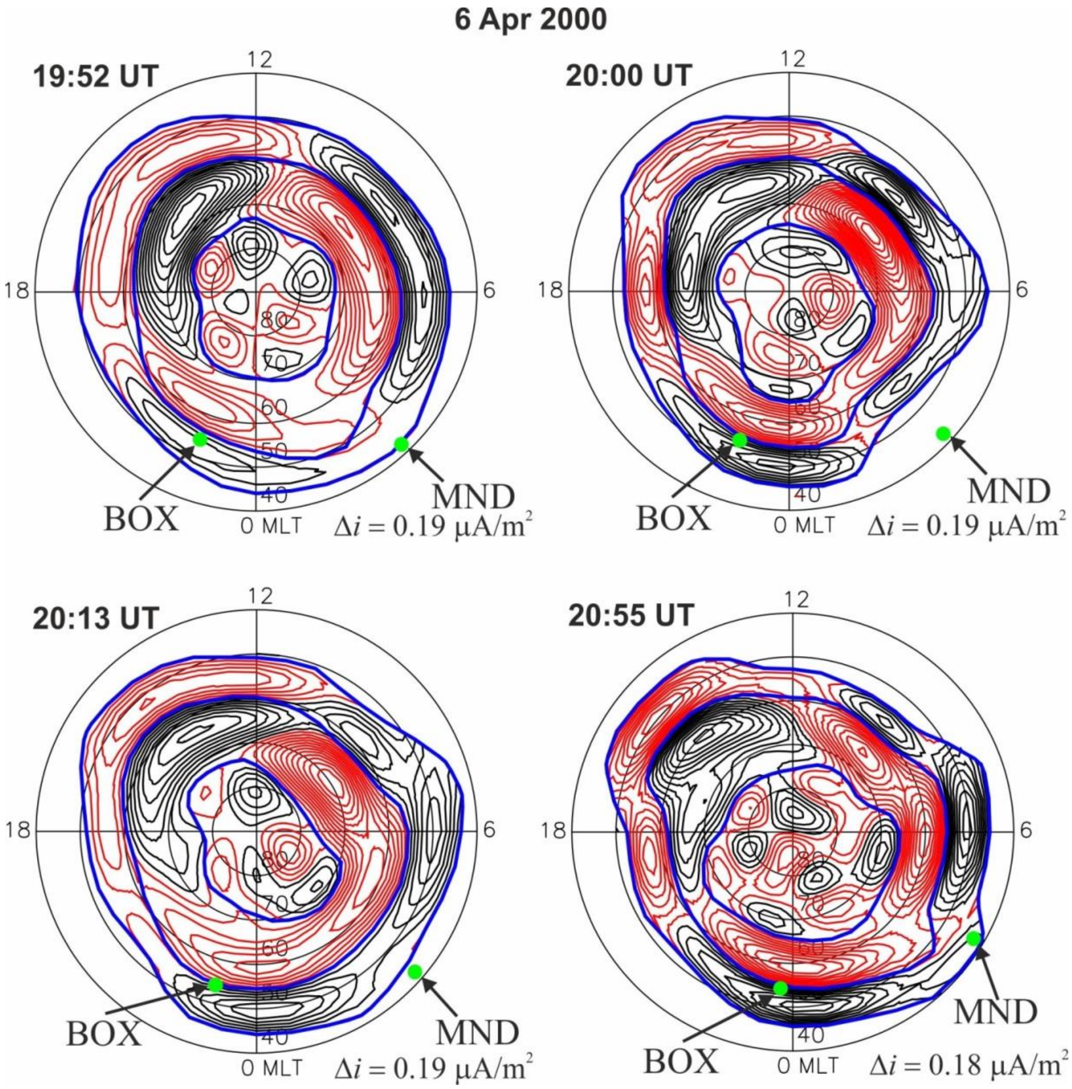

Figure 7. Four moments during the substorm second activation interval during the 6 April 2000 superstorm. The same format as in Figure 4.

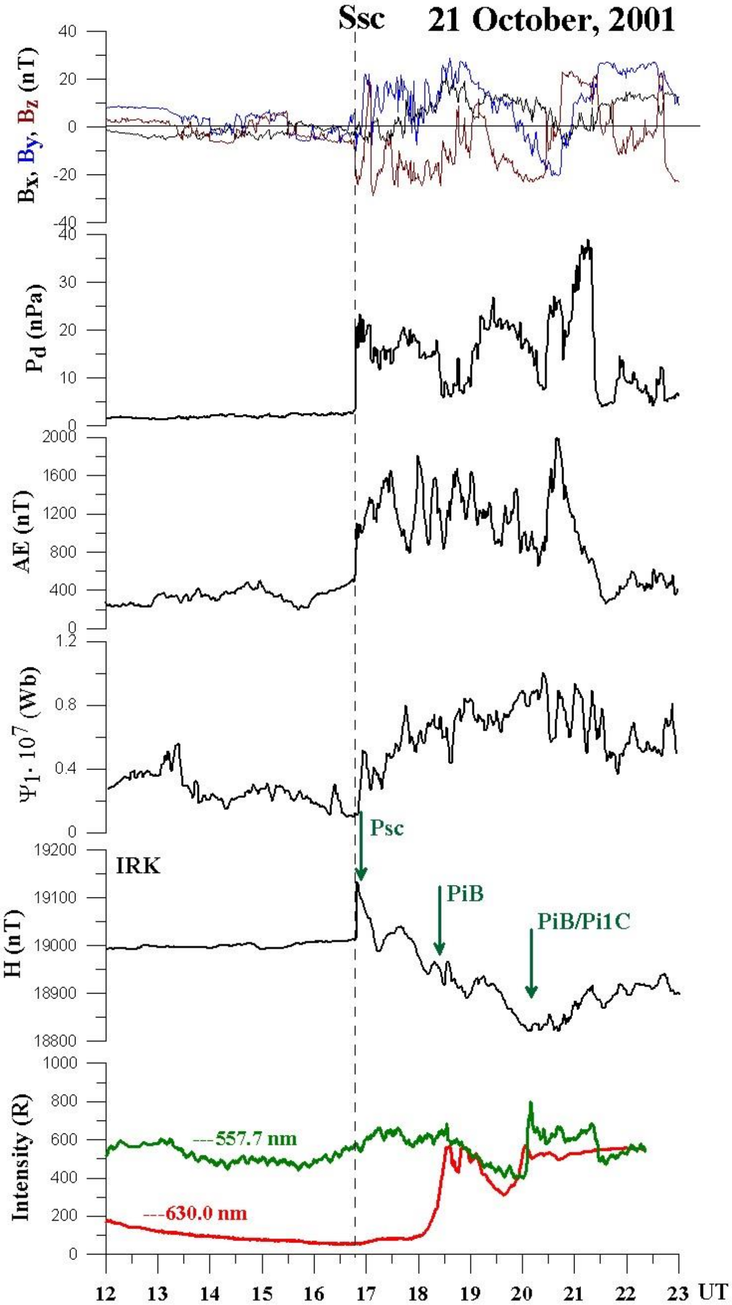

Figure 8. The 21 October 2001 storm. Variations in the IMF components, SW ram pressure (P_d), *AE*-index, magnetic flux through the polar cap, Ψ_1, the H-component of the geomagnetic field from IRK, and intensities of the 557.7 nm (green) and 630.0 nm (red) emissions from TOR.

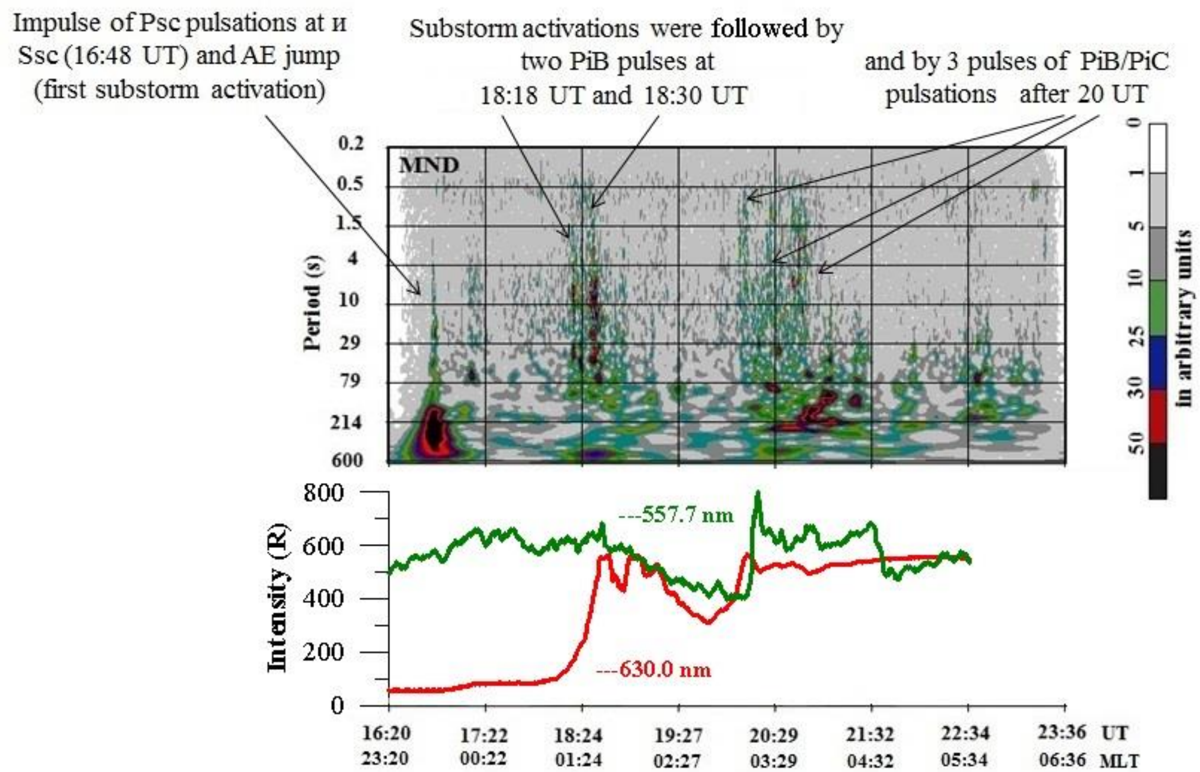

Figure 9. (top) Dynamic spectra of geomagnetic pulsations from MND during the 21 October 2001 storm vs. the pulsation period and UT/MLT. Color codes in arbitrary units for the wave spectrum are given to the right of the spectrogram. (bottom) The intensity of the 557.7 nm (the green line) and 630.0 nm (red) from TOR as a function of UT.

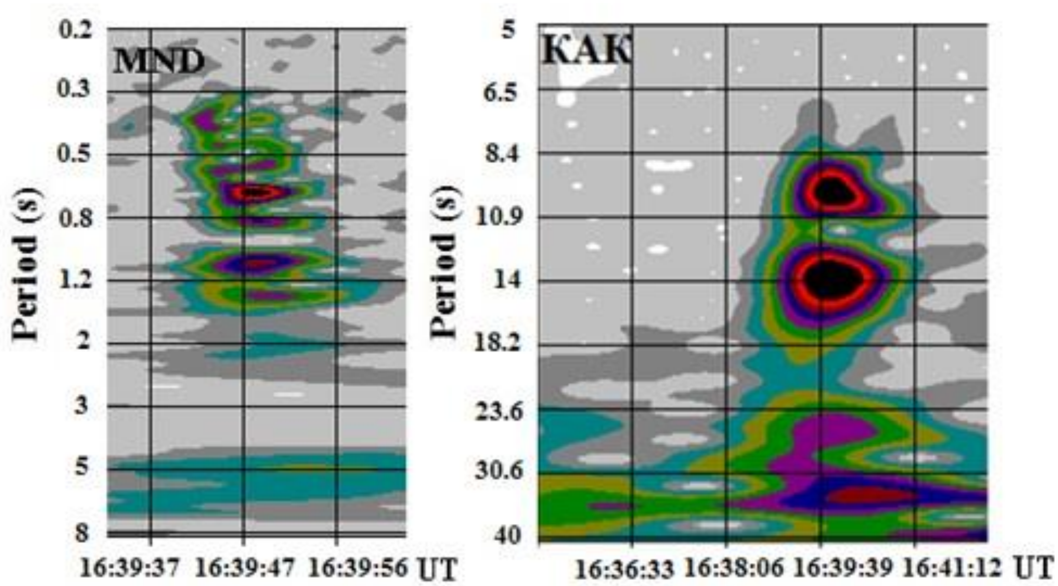

Figure 10. The 6 April 2000 storm. The duration, $\Delta\tau$, of the Psc1, 2 pulsation depending on the sampling rate at MND (10 Hz) and KAK (1 Hz).